# CT and MR evaluation of a wooden foreign body in an in vitro model of the orbit.

J F McGuckin, Jr, N Akhtar, V T Ho, E M Smergel, E J Kubacki and T Villafana

*AJNR Am J Neuroradiol* 1996, 17 (1) 129-133
http://www.ajnr.org/content/17/1/129

# CT and MR Evaluation of a Wooden Foreign Body in an In Vitro Model of the Orbit

J. F. McGuckin, Jr, N. Akhtar, V. T. Ho, E. M. Smergel, E. J. Kubacki, and T. Villafana

**Summary: We made an in vitro model of a wooden foreign body using both fresh and dry pine wood in both fat and soft-tissue background mediums. Air/wood/background medium interfaces were studied with MR and CT to determine which method provided the best image contrast for detecting a wooden foreign body. CT was demonstrated to be superior to MR in the evaluation of the orbit in the in vitro model.**

**Index terms: Foreign bodies; Orbits, computed tomography; Orbits, magnetic resonance**

Detection of an intraorbital wooden foreign body may be difficult, especially in the setting of acute trauma, in which intraorbital emphysema and bone fragments can affect diagnostic accuracy. Confirmation of wood in the orbit depends on the differentiation between wood, soft tissues, and possibly gas or bone. Review of the literature shows successful diagnosis of intraorbital wooden foreign bodies to be variable (1, 2). Standard ophthalmic echography can be highly operator dependent, limited in complete evaluation of the orbit, time consuming, and generally not available in the community setting (3). Researchers have used computed tomography (CT) and magnetic resonance (MR) in the setting of acute penetrating orbital trauma with vastly different outcomes and no consensus (4–9).

## Materials and Methods

We made a model of the orbit in vitro using animal lard to represent orbital fat and 0.9% sodium chloride with 3.5 g/dL human serum albumin to simulate intraorbital muscle tissue or extracellular fluid. Both the fat and extracellular fluid mediums were separately used as background baths in which both fresh and dry pine wood were partially immersed so that a gas/bath/wood interface was created. Axial CT images were obtained with a General Electric (Milwaukee, Wis) 9800 CT Scanner at 120 kV, 120 mA, with a 3-mm section thickness and a 512 × 512 matrix. Images were photographed at window width and level of 80 and 40 Hounsfield units (HU), 214 and 19, 1000 and −500, 1000 and 100, and 4000 and −700.

MR spin-echo pulse sequences including T1-weighted (400/11/2 [repetition time/echo time/excitations]), proton density–weighted (2500/17/2), and T2-weighted (2500/153/2) images were performed on a General Electric Signa 1.5-T scanner using a standard head coil with a section thickness of 3 mm and a 256 × 192 matrix. The window width and level were adjusted to obtain optimal image contrast between the gas, wood, and fat or extracellular medium.

Both CT and MR were performed within 1 hour of immersion of wood. The dry pine wood specimen measured 7 × 3 cm. The freshly cut pine specimen measured 4 cm in diameter.

## Results

CT images of dry pine (Figs 1 and 2) and fresh pine (Figs 3 and 4) were obtained in both air/fat and air/extracellular fluid backgrounds. Dry pine is of very low density and fresh pine more dense as expected; they measure −656 and −24 HU, respectively. The dry pine is best differentiated from gas and fat or extracellular fluid at 1000 and −500 as in Figures 1C and 2C. The dry component of the fresh pine, including the corky bark, annual rings, and pith, behaved much as dry pine. Fresh pine could be best differentiated from gas, fat, and extracellular fluid when a combination of windows 1000 and −500 and 214 and 19 was used, as in Figures 3B and C and 4B and C.

MR imaging with T1-, proton density–, and T2-weighted spin-echo pulse sequences demonstrated both dry and fresh pine wood to be hypointense relative to fat (Figs 5 and 6). Dry pine and both components of fresh pine had

Received November 8, 1994; accepted after revision April 3, 1995.

Presented as a poster at the annual meeting of the Radiological Society of North America, 1993.

From the Department of Diagnostic Imaging, Temple University Hospital, Philadelphia.

Address reprint requests to J. F. McGuckin, Jr, MD, 419 Spring Mill Rd, Villanova, PA 19085-1925.

AJNR 17:129–133, Jan 1996 0195-6108/96/1701–0129 

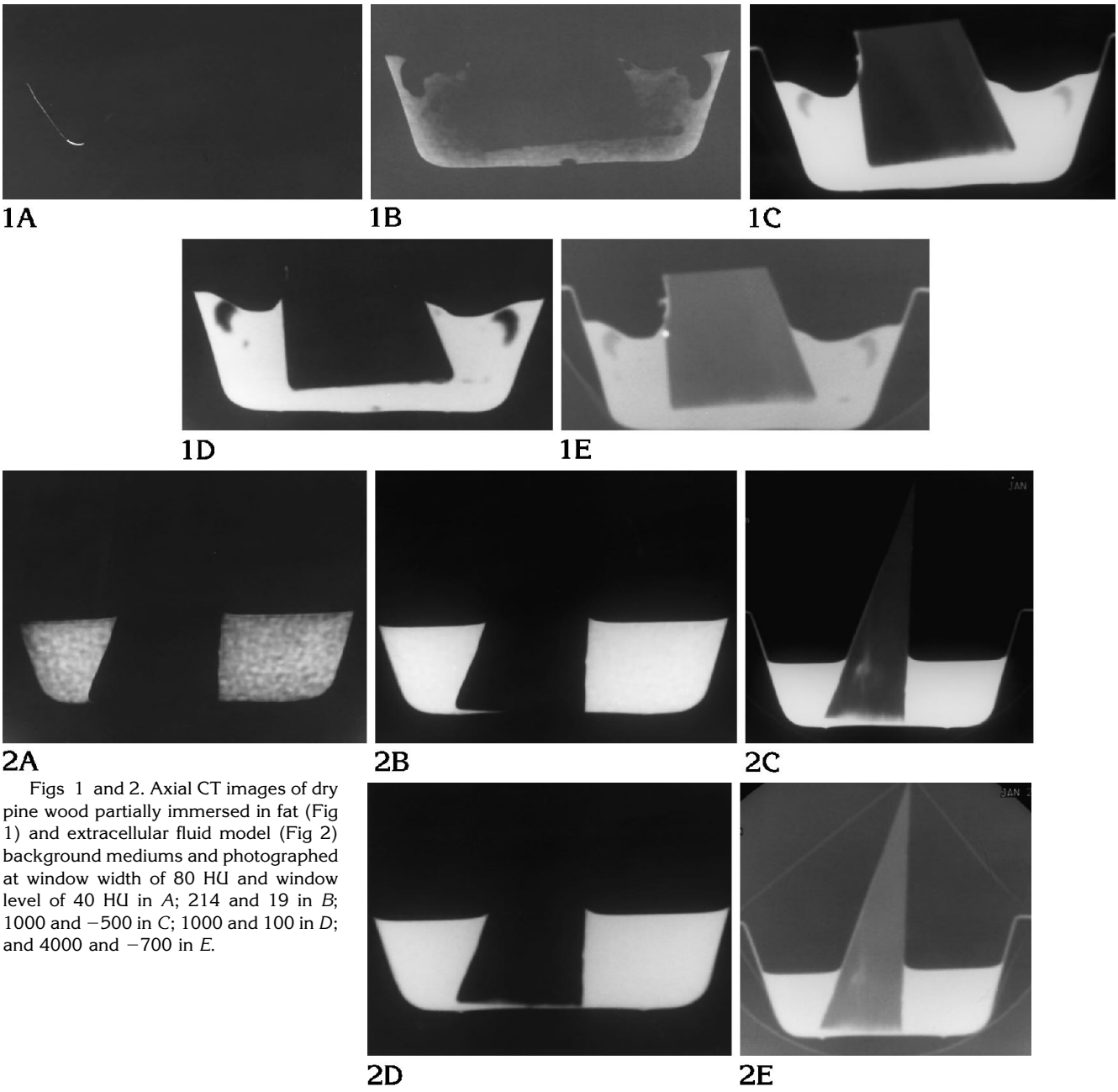


Figs 1 and 2. Axial CT images of dry pine wood partially immersed in fat (Fig 1) and extracellular fluid model (Fig 2) background mediums and photographed at window width of 80 HU and window level of 40 HU in *A*; 214 and 19 in *B*; 1000 and −500 in *C*; 1000 and 100 in *D*; and 4000 and −700 in *E*.

good image contrast relative to both the fat and extracellular fluid background mediums. MR, however, did not differentiate dry pine and the dry component of fresh pine from gas regardless of window width and level variation.

## Discussion

Wood evaluated with CT has been described as an area of low or high attenuation relative to fat depending on the degree of its air or water content. It can also mimic air within the orbit. Often, the presence of a wooden foreign body in the orbit is inferred secondary to a geometrical interface between the area of low attenuation and soft tissues (3–7). Measurement of absorption coefficients was not thought to be helpful in distinguishing small pieces of wood from air because of volume averaging. Our experiment demonstrated that window width and level variation are extremely useful in differentiating wood from gas, fat, and extracellular fluid.

MR revealed that both dry and fresh wood are hypointense relative to intraorbital fat on all

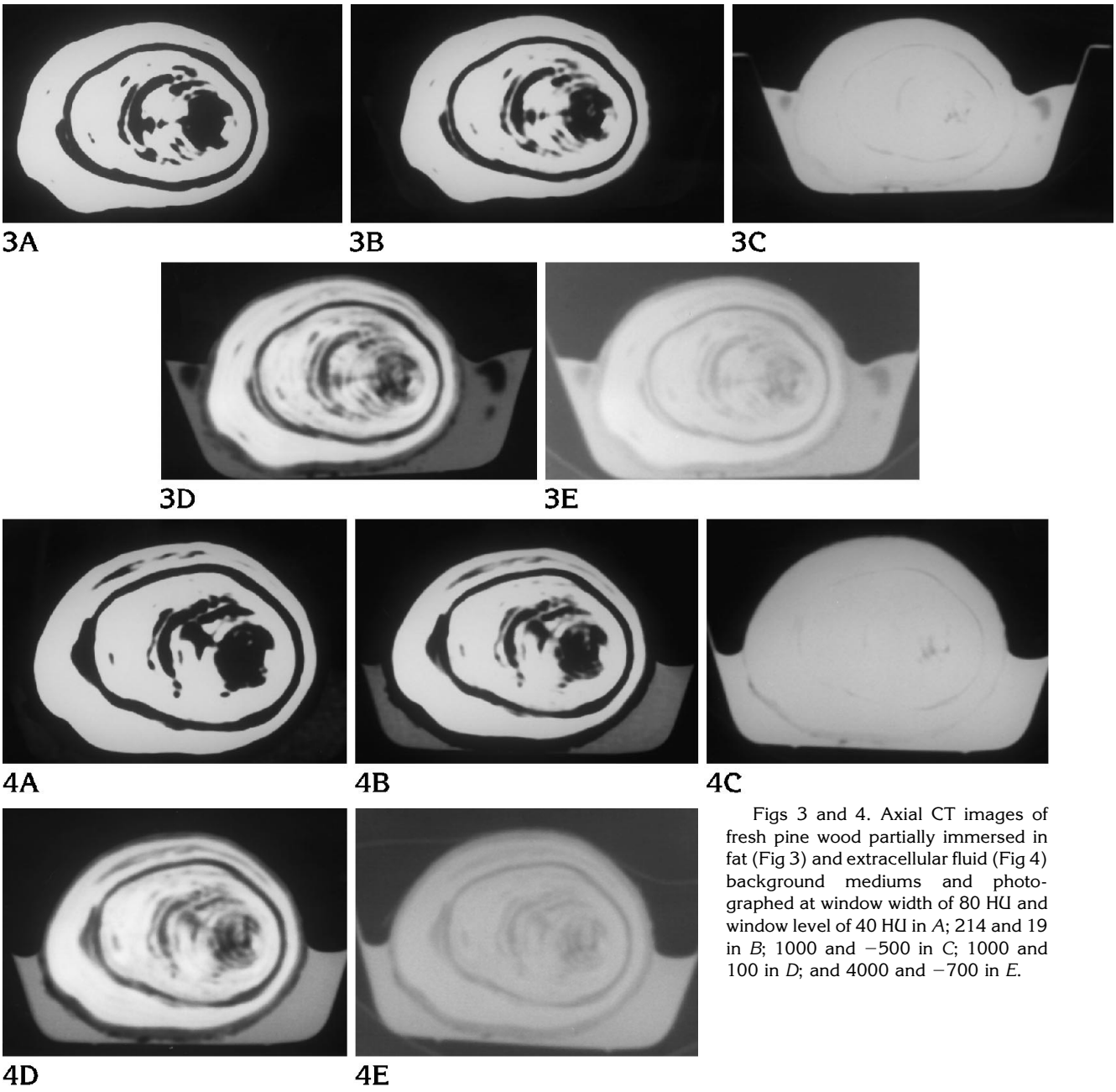


Figs 3 and 4. Axial CT images of fresh pine wood partially immersed in fat (Fig 3) and extracellular fluid (Fig 4) background mediums and photographed at window width of 80 HU and window level of 40 HU in *A*; 214 and 19 in *B*; 1000 and −500 in *C*; 1000 and 100 in *D*; and 4000 and −700 in *E*.

spin-echo pulse sequences. This has been demonstrated in our experiment. The hypointensity of dry wood with its high air content and fresh wood with its high water content is probably attributable to the lack of mobile protons. T1-weighted spin-echo images have been favored over proton density– and T2-weighted spin-echo images, because they provide better contrast between fat and wood. In addition, they may decrease motion artifact by requiring less imaging time.

CT and MR can be used to discriminate dry and fresh pine wood from fat and extracellular fluid backgrounds. In this study, although fresh pine was slightly better seen on MR than CT, MR did not differentiate dry wood and the dry component of fresh wood from air or bone fragments, which can be encountered in the setting of penetrating orbital trauma. CT with optimization of image contrast through proper windowing can differentiate dry and fresh wood from air and bone fragments and is therefore the imag-

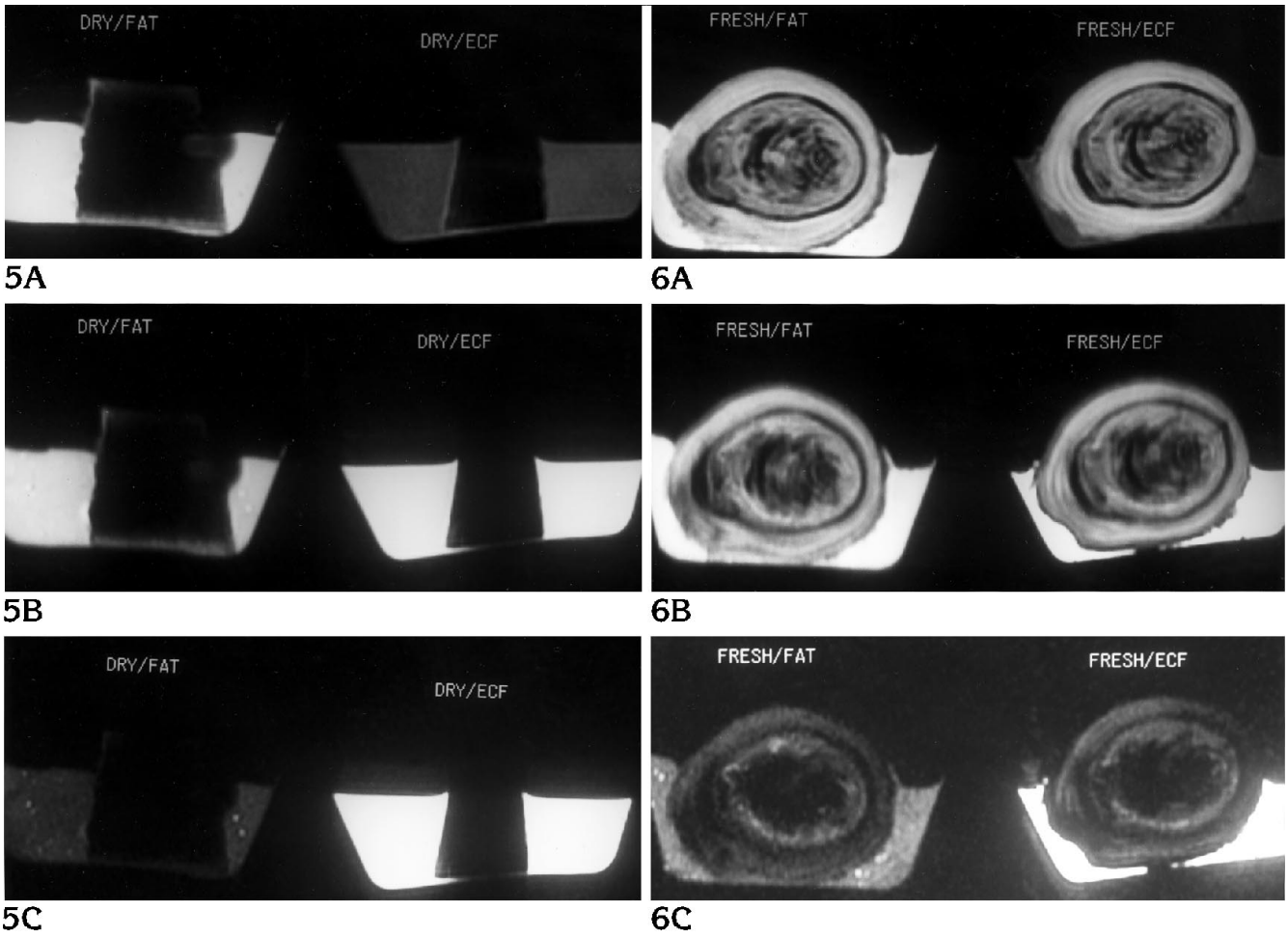


Figs 5 and 6. MR spin-echo pulse sequences including T1-weighted (400/11/2)(*A*), proton density–weighted (2500/17/2) (*B*), and T2-weighted (2500/153/2) (*C*) axial images of dry (Fig 5) and fresh (Fig 6) pine wood.

ing modality of choice. CT has the advantage of not being restricted when a metallic foreign body is present. Moreover, CT is less expensive, more readily available, and faster to perform than MR.

There are some variables that were not addressed in this study. We evaluated only fresh and dry pine specimens, but different types of wood have been shown to have varying densities and water content (10, 11). Additionally, wood surface coatings such as paint or dirt or the immersion time of the piece of wood in its respective bath (extracellular fluid/fat) may also change the imaging characteristics (10–13). The size of the wood chip is also important, because there may be a disparity in attenuation coefficients if a smaller piece of wood is used because of partial volume averaging (14). Finally, only T1-, proton density–, and T2-weighted spin-echo sequences were performed; other sequences such as fast spin-echo, fat-suppressed, or short-tau inversion recovery may provide additional information, especially related to the varying water content of wood. We are currently undertaking a study to evaluate the effects of wood specimen size, specimen immersion time, and different types of wood with common surface coatings such as paint using various pulse sequences on MR.

In conclusion, thin axial and coronal CT images at various window widths should be used as the first imaging modality to detect intraorbital wood foreign bodies. Although MR does not show an advantage over CT in our study, further investigation is required to assess its role fully.

## References


1. Green BF, Kraft SP, Carter KD, Buncic JR, Nerad JA, Armstrong D. Intraorbital wood: detection by magnetic resonance imaging. *Ophthalmology* 1990;97:608–611
2. Ossoinig KC. Detection of wood foreign bodies (letter). *Ophthalmology* 1991;98:274
3. Green BF, Kraft SP. Letter. *Ophthalmology* 1991;98:274–275
4. Zentner J, Hassler W, Petersen D. A wooden foreign body penetrating the superior orbital fissure. *Neurochirurgia* 1991;34:188–190
5. Glatt HJ, Custer PL, Barrett L, Sartor K. Magnetic resonance imaging and computed tomography in a model of wooden foreign bodies in the orbit. *Ophthalm Plast Reconstr Surg* 1990;6:108–114
6. Wilson WB, Dreisbach JN, Lattin DE, Stears JC. Magnetic resonance imaging of nonmetallic orbital foreign bodies. *Am J Ophthalmol* 1988;105:612–617
7. Roberts CF, Leehey PJ III. Intraorbital wood foreign body mimicking air at CT. *Radiology* 1992;185:507–508
8. Specht CD, Varga JH, Jalali MM, Edelstein JP. Orbitocranial wooden foreign body diagnosed by magnetic resonance imaging: dry wood can be isodense with air and orbital fat by computed tomography. *Surv Ophthalmol* 1992;36:341–344
9. Woolfson JM, Wesley RE. *Ophthalm Plast Reconstr Surg* 1990;6: 237–240
10. Hansen JE, Gudeman SK, Holgate RC, Saunders RA. Penetrating intracranial wood wounds: clinical limitations of computerized tomography. *J Neursurg* 1988;68:742–756
11. Kadir S, Aronow S, Davis KR. The use of computerized tomography in the detection of intra-orbital foreign bodies. *Comput Tomogr* 1977;1:151–156
12. Kuhns LR, Borlaza GS, Seigel RS, Paramagul MO, Berger PE. An in vitro comparison of computed tomography, xeroradiography, and radiolgraphy in the detection of soft-tissue foreign bodies. *Radiology* 1979;132:218–219
13. Weisman RA, Savino PJ, Schut L, Schatz NJ. Compted tomography in penetrating wounds of the orbit with retained foreign bodies. *Arch Otoloaryngol* 1983;109:265–268
14. Tate E, Cupples H. Detection of orbital foreign bodies with computed tomography: current limits. *AJR Am J Roentgenol* 1981; 137:493–495